Top-down control analysis of temperature effect on oxidative phosphorylation

Sylvie DUFOUR, Nicole ROUSSE, Paul CANIONI and Philippe DIOLEZ*

Résonance Magnétique des Systèmes Biologiques, UMR 9991, CNRS/Bordeaux 2, 146 rue Léo-Saignat, F-33076 Bordeaux cedex, France

The effects of temperature on the control of respiration rate, phosphorylation rate, proton leakage rate, the protonmotive force and the effective ATP/O ratio were determined in isolated rat liver mitochondria over a range of respiratory conditions by applying top-down elasticity and control analyses. Simultaneous measurements of membrane potential, oxidation and phosphorylation rates were performed under various ATP turnover rates, ranging from state 4 to state 3. Although the activities of the three subsystems decreased with temperature (over 30-fold between 37 and 4 °C), the effective ATP/O ratio exhibited a maximum at 25 °C, far below the physiological value. Top-down elasticity analysis revealed that maximal membrane potential was maintained over the range of temperature studied, and that the proton leakage rate was considerably reduced at 4 °C. These results definitely rule out a possible uncoupling of mitochondria at low temperature. At 4 °C, the decrease in ATP/O ratio is explained by the relative decrease in phosphorylation processes revealed by the decrease in depolarization after ADP addition [Diolez and Moreau (1985) Biochim. Biophys. Acta **806**, 56–63]. The change in depolarization between 37 and 25 °C was too small to explain the decrease in ATP/O ratio. This result is best explained by the changes in the elasticity of proton leakage to membrane potential between 37 and 25 °C, leading to a higher leak rate at 37 °C for the same value of membrane potential. Top-down control analysis showed that despite the important changes in activities of the three subsystems between 37 and 25 °C, the patterns of the control distribution are very similar. However, a different pattern was obtained at 4 °C under all phosphorylating conditions. Surprisingly, control by the proton leakage subsystem was almost unchanged, although both control patterns by substrate oxidation and phosphorylation subsystems were affected at 4 °C. In comparison with results for 25 and 37 °C, at 4 °C there was evidence for increased control by the phosphorylation subsystem over both fluxes of oxidation and phosphorylation as well as on the ATP/O ratio when the system is close to state 3. However, the pattern of control coefficients as a function of mitochondrial activity also showed enhanced control exerted by the substrate oxidation subsystem under all intermediate conditions. These results suggest that passive membrane permeability to protons is not involved in the effect of temperature on the control of oxidative phosphorylation.

INTRODUCTION

The physical properties of biological membranes are of functional significance and under physiological control. The purpose of this study was to investigate their role (via the proton conductance of the mitochondrial inner membrane) in the control of oxidative phosphorylation by varying the temperature. Top-down control analysis was used because it seemed the most convenient tool to discriminate between the various effects of temperature modification. The literature is poorly documented on the effect of low temperature on oxidative phosphorylation in isolated mitochondria [1–6]. The studies published so far have concluded that there is a decrease in oxidative phosphorylation efficiency with temperature from 25 to 10 °C [5,6]. A loss of mitochondrial membrane integrity at low temperature has been discounted but no clear explanation has been proposed [6]. However, no measurement of proton leakage has so far been performed under these conditions and the effect of low temperature on oxidative phosphorylation itself is still unclear, as well as the decrease in phosphorylation efficiency observed between 25 and 37 °C [6]. The first insight from the present study is the measurement of membrane potential to investigate the internal membrane conductance to protons and to further document its exact role on phosphorylation efficiency and control of distribution in oxidative phosphorylation.

These questions were investigated by top-down control analysis, an efficient method that provides an immediate overview of the control structure of the whole pathway under investigation [7–9]. This approach groups the system into two or three subsystems of reactions connected by a common intermediate [10]. It was first applied to determine the control of oxidative phosphorylation in animal [7,8,11,12] or plant mitochondria [13,14] under variable phosphorylating conditions. In those studies, the kinetic responses of substrate oxidation, the phosphorylation reactions and proton leakage to their common intermediate (the protonmotive force, Δp) were measured under different ATP turnover conditions. This analysis also offers the opportunity to study the distribution of control on complex functions [15], for example the ATP/O ratio [16]. In the present study we took advantage of the capabilities of the top-down approach to investigate the effect of complex modulators on a system. Indeed, it has been successfully applied to discriminate between the different effects of thyroid hormones on hepatocytes [9,17,18]. Recent papers also show its use to discriminate between the various poisonous effects of heavy metals on mitochondrial functions [19–21].

Abbreviations used: Δp, protonmotive force; $\Delta\Psi$, membrane potential; ΔpH, pH gradient across the mitochondrial inner membrane; J_c, rate of oxygen consumption by the respiratory chain reactions; J_l, rate of oxygen consumption required to pump protons out at the rate equal to the rate of proton entry through proton leakage; J_p, rate of ATP synthesis; $C_i^{J_i}$, overall control coefficient of subsystem i over J_i (J_c, J_l or J_p) or $\Delta\Psi$ or ATP/O ratio; $\epsilon^i_{\Delta\Psi}$, overall elasticity of subsystem i to $\Delta\Psi$; RC, respiratory control; TPP^+, tetraphenylphosphonium ion.

* To whom correspondence should be addressed.

The effect of temperature – a typical complex effector – on an integrated system such as oxidative phosphorylation is quite complex to assess, because temperature has different effects on the different enzyme subsystems as well as on membrane properties. There were two stages in this study: first we applied top–down elasticity analysis to characterize temperature effects on the inner mitochondrial membrane conductance to protons; secondly we measured control coefficients to quantify the control exerted by the system parameters (subsystems) over the values taken by the system variables (fluxes, fluxes ratio and the value of Δp). These analyses were carried out at different temperatures on isolated rat liver mitochondria oxidizing succinate at various ATP turnover rates.

EXPERIMENTAL

Preparation of rat liver mitochondria

Male Wistar rats (8 weeks old, average weight 200 g) were killed by cervical dislocation and liver was removed and homogenized in ice-cold sucrose buffer [0.3 M sucrose, 5 mM Tes, 0.2 mM EGTA , 1 % (w/v) BSA, pH 7.2]. Mitochondria were isolated by the method of Cannon and Lindberg [22] and kept on ice in sucrose buffer.

Simultaneous monitoring of respiration rate, membrane potential and phosphorylation rate

Oxygen consumption, membrane potential and ATP synthesis were determined simultaneously in a glass vessel (final volume 3 ml) in a medium containing 100 mM KCl, 40 mM sucrose, 10 mM KH_2PO_4, 5 mM $MgCl_2$, 1 mM EGTA, 1 % (w/v) BSA, pH 7.2, and 5 μM rotenone. Mitochondrial protein concentration in the vessel varied from 250 μg/ml (37 and 25 °C) to 1.2 mg/ml (4 °C). Mitochondrial concentration was 2.4 mg/ml for proton leakage measurements at 4 °C after control of the absence of effect of protein concentration on the results (results not shown). Succinate (5 mM) was used as substrate. Further additions are detailed in the figures. Oxygen uptake was measured polarographically with a Clark type electrode (Rank Brothers), pH changes with a sensitive pH electrode. Membrane potential was followed by using a laboratory-constructed tetraphenylphosphonium (TPP^+)-sensitive electrode coupled to a remote Ag/AgCl-saturated reference electrode.

Respiration rates were calculated with respect to calibration of the oxygen electrode with air-saturated medium containing 220 μM O_2 at 37 °C, 240 μM O_2 at 25 °C and 385 μM O_2 at 4 °C [23].

Membrane potential ($\Delta\Psi$) was calculated by using the equation of Kamo et al. [24]:

$$\Delta\Psi = (RT/F)\log(v/V) - (RT/F)\log(10^{\Delta E/(RT/F)} - 1) \quad (1)$$

where v is the mitochondrial matrix volume, V is the volume of the measurement medium and ΔE is the deflection of the TPP^+ electrode from the baseline, derived from the calibration of the electrode. The mitochondrial matrix volume was taken as 1.21 μl per mg of protein, according to Goubern et al. [25]. The calibration of the TPP^+ electrode consisted of doubling the TPP^+concentration (from 3 to 6 μM) before the addition of mitochondria. Non-specific TPP^+ binding was accounted for by subtracting 50 mV from all measured $\Delta\Psi$ values [25]. It was apparent that ΔpH was relatively constant (about 5–10 mV) at 25 °C, under different conditions of phosphorylation in 10 mM phosphate-containing buffer [9]. This value was not different from the mitochondrial–cytosolic pH gradient, measured by NMR spectroscopy, on a whole rat liver perfused at 4 °C [26].

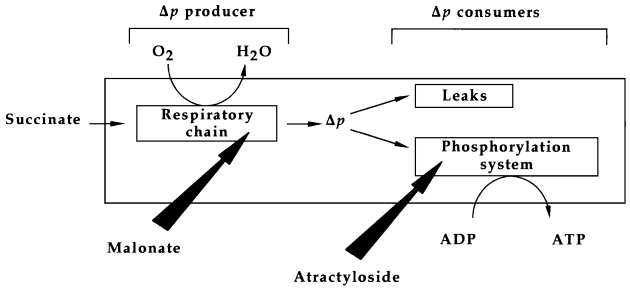

Figure 1 Scheme of oxidative phosphorylation in rat liver mitochondria

The system consists of all the steps within the box and is divided into three subsystems of reactions (inner boxes); the three subsystems are connected by the common thermodynamic intermediate (Δp). The ADP–atractyloside system was used to maintain intermediate phosphorylation rates, and malonate titrations were carried out for the determination of elasticity coefficients.

ΔpH was negligible compared with measured membrane potentials (180 mV as average value) and do not appear very different at 4 °C. Membrane potential was therefore a suitable parameter for this study, especially because it was continuously measured in our experimental device. The low value of ΔpH does not interfere with control analysis as fractional changes are used for elasticity and control analyses (see below). State 3 membrane potential values reported below in Figure 3 are the lowest values obtained after ADP addition, usually during the second addition. The values obtained were similar to those obtained after addition of a saturating ADP concentration for control analysis experiments.

The pH changes were converted into H^+ consumption by titrating the suspension with titrated HCl at the end of the kinetics. HCl injections also showed that the time response of the pH electrode was never rate-limiting for kinetic studies. H^+ consumption was converted into ATP synthesis by using the following equilibrium [27]:

$$ADP^{q-} + P_i^{r-} + mH^+ \rightarrow ATP^{p-} + H_2O \quad (2)$$

with $m = q + r - p$. The value of m was calculated for all experiments from the total proton consumption measured after phosphorylation of a known amount of ADP. Conditions were chosen so that the pH variation never exceeded 0.1 for the whole range of the kinetics.

Protein determination

Mitochondrial protein concentration was determined by the Bradford method [28].

Top-down analysis

Following previous use [13] of top-down metabolic control analysis [8], we divided the system of oxidative phosphorylation into the following three subsystems linked by the common intermediate Δp: the substrate oxidation subsystem producing Δp (substrate translocases, dehydrogenases, respiratory chain complexes) and the two subsystems that consume the Δp, either coupled to ATP synthesis (the phosphorylation subsystem, including the ATP synthase and the ATP/ADP-translocase and the phosphate translocase) or without ATP synthesis (proton leakage subsystem including the passive permeability of the mitochondrial inner membrane to protons, and any cation cycling reactions) (Figure 1).

Complete top-down control analysis requires the measurement of the fluxes through the different subsystems, and determination of the corresponding elasticity coefficients over Δp for every condition of phosphorylation studied. The fluxes through substrate oxidation (J_c) and phosphorylation (J_p) subsystems were measured simultaneously with the determination of membrane potential. Proton leakage flux (J_l) was calculated for the same value of membrane potential from independent titration curves (see below). Appropriate titrations of the different fluxes were carried out to determine the elasticities of the three subsystems to Δp and the control coefficients of the respiratory chain, the phosphorylation system and proton leakage over each flux, over the value of Δp and the ATP/O ratio.

Determination of overall elasticity coefficients to $\Delta\Psi$

The overall elasticities of the chain, proton leakage and phosphorylation subsystems to protonmotive force were calculated as described by Hafner et al. [8]. Determination of the elasticity of a subsystem to the protonmotive force consists of modifying Δp by an adequate titration of a subsystem that differs from the subsystem under consideration. This analysis has been performed for different conditions of ATP synthesis set up by using various atractyloside concentrations in the presence of excess ADP. The hexokinase–glucose system could not be used for these studies because the balance of H^+ is null under these phosphorylating conditions. For every ATP turnover set up, the different fluxes have been measured under steady-state conditions; i.e. when a true constant value of $\Delta\Psi$ was obtained.

The elasticity of the respiratory chain (Δp-producing subsystem) to Δp was obtained from the titration of the phosphorylation system (Δp-consuming subsystem) with atractyloside: the addition of increased concentrations of inhibitor induces increased steady-state values of Δp that cause reajustments of the flux through the respiratory chain. The elasticity of the respiratory chain in any phosphorylating condition is defined as the ratio between the fractional change in the respiration flux (dJ_c/J_c) and the fractional change in Δp ($d\Delta p/\Delta p$), approximated to the fractional change in $\Delta\Psi$ ($d\Delta\Psi/\Delta\Psi$). Elasticity coefficients can be determined from the plot of J_c against $\Delta\Psi$ obtained during atractyloside titration and corresponds to the normalized slope of the titration curve multiplied by $\Delta\Psi/J_c$:

$$\epsilon^{J_c}_{\Delta\Psi} = (dJ_c/d\Delta\Psi).(\Delta\Psi/J_c) \quad (3)$$

The elasticity of proton leakage to Δp was obtained from the titration of the Δp-producing subsystem with malonate in the absence of phosphorylation (using 0.5 μg of oligomycin per mg of protein). Under these conditions, the flux through the respiratory chain under steady-state conditions exactly matches the proton leakage flux (the only Δp consumer). The elasticity of proton leakage to Δp corresponds to the ratio between the fractional change in the proton leakage flux (expressed as equivalent oxygen consumption) and the fractional change in Δp (i.e. to the normalized slope of the malonate titration curve multiplied by $\Delta\Psi/J_l$) from the plot of J_l against $\Delta\Psi$:

$$\epsilon^{J_l}_{\Delta\Psi} = (dJ_l/d\Delta\Psi).(\Delta\Psi/J_l) \quad (4)$$

The main improvement in the study presented here over all previous reports is that the elasticity of phosphorylation subsystem to Δp under all phosphorylating conditions was directly determined during the titration of respiratory chain by malonate. The fractional change in the flux of phosphorylation (dJ_p/J_p) divided by the fractional change in Δp allows the direct calculation of the overall elasticity to Δp (without any correction for proton leakage), because J_p was measured simultaneously by using a pH-sensitive electrode. At a given $\Delta\Psi$ the elasticity coefficient corresponds to the normalized slope of phosphorylation rate (at a given concentration of atractyloside) during malonate titration, multiplied by $\Delta\Psi/J_p$:

$$\epsilon^{J_p}_{\Delta\Psi} = (dJ_p/d\Delta\Psi).(\Delta\Psi/J_p) \quad (5)$$

where $\Delta\Psi$ is the membrane potential, J_c is the flux through the respiratory chain, J_l is the flux through the proton leakage branch (both expressed as rates of oxygen consumption) and J_p is the flux through the phosphorylation branch (expressed as the rate of ATP synthesis).

Determination of overall control coefficients

Overall control coefficients are defined as the fractional change in flux (flux control coefficient) or in Δp (concentration control coefficient) in response to an infinitesimal change in the activity of the subsystem under consideration.

Overall flux control coefficients were calculated in every phosphorylating condition from the overall elasticities by using the 12 equations given in Hafner et al. [8], and those derived from the summation theorems, the connectivity property [29,30] and the branching theorem of metabolic control analysis [31]. The equations include here the stoichiometric coefficient for the expression of J_p as oxygen consumption on the basis of the now generally accepted value of 1.5 for the mechanistic (maximal) ATP/O ratio for succinate oxidation [16].

Determination of control coefficients over the effective ATP/O ratio

Control coefficients over the value of the effective ATP/O ratio were determined from the same data set. The effective ATP/O ratio is the amount of total ATP produced per total oxygen consumed (expressed as n-atoms of O). Therefore the control coefficient of each subsystem over the effective ATP/O ratio is given by [15,16]:

$$C_i^{ATP/O} = C_i^{J_p} - C_i^{J_c} \quad (6)$$

where i represents the different subsystems.

RESULTS AND DISCUSSION

Effect of temperature on oxidative phosphorylation

The effect of temperature on the parameters of mitochondrial activity was first assessed by a classical study of oxidative phosphorylation, by using simultaneous measurements of oxygen consumption, membrane potential and phosphorylation rate. The same device was used later for the elasticity and control analyses.

Typical experimental traces recorded at 4, 25 and 37 °C are presented in Figure 2. The general features were the same for all temperatures studied. After calibration of the TPP^+-sensitive electrode with increasing concentrations of TPP^+, addition of mitochondria induced a decrease in TPP^+ concentration in the medium, indicating TPP^+ uptake by mitochondria in response to the generation of a transmembrane potential, probably owing to the presence of endogenous respiratory substrates. Subsequent addition of succinate caused the onset of oxygen uptake and a further increase in membrane potential. The addition of a limiting amount of ADP resulted in a concomitant increase in oxidation rate and a decrease in membrane potential (state 3), owing to the

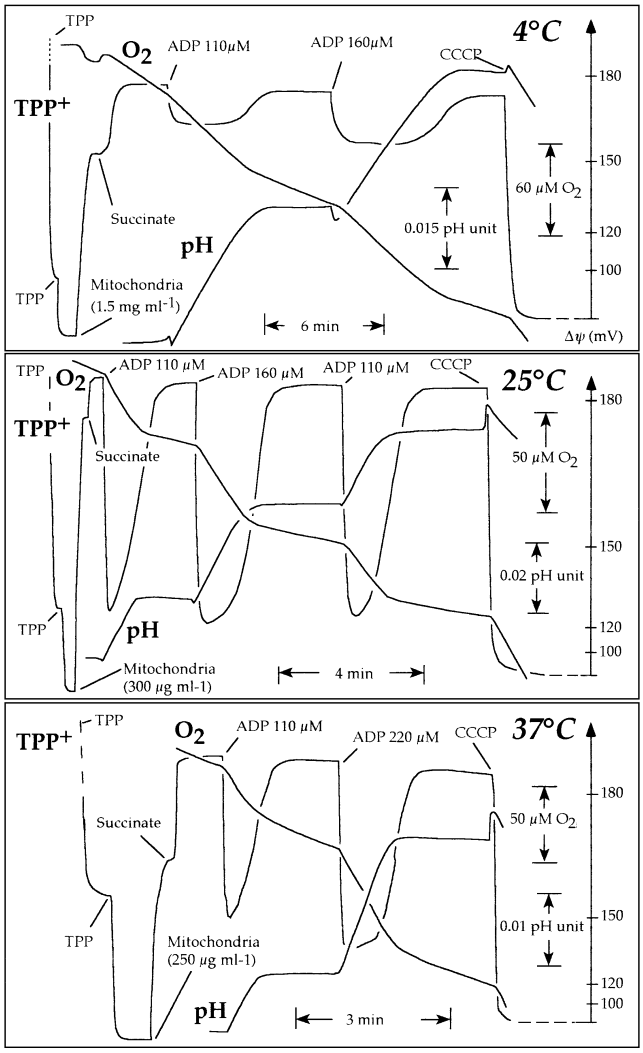

Figure 2 Simultaneous recordings of respiration, membrane potential and pH changes at different temperatures

Assays were performed at 4, 25 and 37 °C as described in the Experimental section. Respiration was initiated by the addition of 5 mM succinate. Final uncoupling was obtained by addition of 2.5 μM carbonyl cyanide *m*-chlorophenylhydrazone; further additions are detailed on each trace.

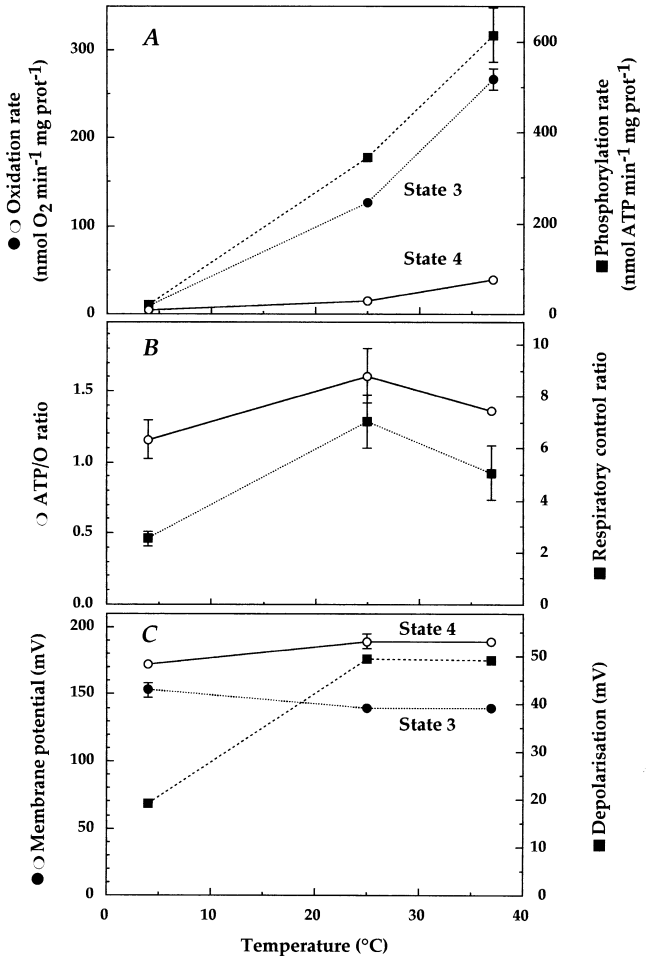

Figure 3 Temperature dependence of various energetic parameters

Every data point represents the mean ± S.D. for at least eight assays (from a total of ten independent mitochondrial preparations). (**A**) Respiratory rates were measured in the absence (state 4, ○) or in the presence (state 3, ●) of ADP (see Figure 2); the corresponding phosphorylation rates are also recorded (■). (**B**) ATP/O (○) and respiratory control (■) ratios were calculated from experiments similar to those presented in Figure 2. (**C**) Membrane potential values were measured under state 4 (○) and state 3 (●) conditions; the resulting depolarizations (state 4 minus state 3, ■) are also recorded.

onset of phosphorylation, as measured by the pH electrode [27]. After phosphorylation of added ADP, the decrease in oxidation rate was associated with an increase in membrane potential; both returned to the values obtained after succinate addition (state 4). The addition of an uncoupler (carbonyl cyanide *m*-chlorophenylhydrazone) caused the collapse of the membrane potential and the complete release of TPP^+ from the mitochondria.

Under the conditions used for the control analysis, simultaneous measurement of the different parameters was very useful for the calculation of oxidative phosphorylation force and fluxes in a stationary state. These conditions were obtained by addition of ADP at a saturating concentration, and measurements were made after a constant membrane potential had been obtained.

Experiments similar to those presented in Figure 2 allow the variation of the different parameters of oxidative phosphorylation to be studied as a function of temperature (Figure 3). Figure 3A illustrates the rapid increase in the oxidation rate with temperature, both in state 3 and in state 4. A similar variation was observed for ATP synthesis rate (Figure 3A). We observed a halving in oxidation and phosphorylation rates between 37 and 25 °C, and a large, unexpected decrease to one-tenth between 25 and 4 °C. The oxidative phosphorylation efficiency (ATP/O ratio) and the respiratory control (RC) ratio were also calculated (Figure 3B). In contrast with oxidation and phosphorylation rates, these parameters exhibited a maximum at 25 °C. The increase in ATP/O and RC ratios between 37 and 25 °C is quite surprising (see also [6]) and the validity of these ratios as unequivocal criteria of mitochondrial integrity may be questioned. Therefore, in comparison with 25 °C, mitochondria present a lower phosphorylation efficiency, indicating a possible uncoupling, either at 37 °C or at 4 °C.

Additional information was drawn from the measurements of membrane potential values with the TPP^+-sensitive electrode

(Figure 3C). The membrane potential value is maximal under state 4 conditions and reflects directly the mitochondrial inner membrane integrity. Comparable results were obtained at 25 and 37 °C (mean 189 mV), and only a slight decrease (9%) was observed at 4 °C (173 mV) (Figure 3C). Therefore this homoeostasis of membrane potential strongly suggests that the lower ATP/O and RC ratios at 4 or 37 °C are not the consequence of mitochondrial uncoupling. In contrast, changes in state 3 membrane potential values presented a very different picture. Whereas these values were also identical at 25 and 37 °C (140 mV), an increase was observed at 4 °C (153 mV). Therefore the main effect of temperature on membrane potential was observed on depolarization (change in membrane potential in response to ADP addition), which showed a large dependence on temperature between 25 and 4 °C (Figure 3C). The decrease in depolarization in this temperature range reveals a relative inhibition of the phosphorylation subsystem activity, as already described by Diolez and Moreau [32], consistent with the decrease in ATP/O and RC ratios. Effectively no change in depolarization was observed during progressive uncoupling, and an increase was observed during progressive inhibition of the respiration subsystem [32]. The apparent uncoupling at 4 °C is the direct consequence of the increase in membrane potential in state 3, leading to an increase in proton leakage. The same explanation cannot be used for the decrease in oxidative phosphorylation at 37 °C, as the same values of membrane potential were observed at 25 °C and at 37 °C. Although true uncoupling may be discarded in all conditions from the measurements of mitochondrial membrane potential, it is clear that the mechanism responsible for the decrease in phosphorylation efficiency is different at 37 °C and at 4 °C.

Top-down elasticity analysis of proton leakage

The above results suggested a possible modification of proton leakage with temperature. The protonmotive force is the obligatory intermediate between the different subsystems of oxidative phosphorylation; it is produced by the reactions of substrate oxidation and consumed by two types of processes linked (phosphorylation) or not (proton leakage) to ATP synthesis (see Figure 1). Proton leakage short-circuits phosphorylation and its evolution is of fundamental importance in the effective oxidative phosphorylation efficiency. We showed previously that proton leakage is dependent only on the protonmotive force and not on mitochondrial activity [33]. Therefore the activity of proton leakage is represented by the relationship between oxygen consumption and $\Delta\Psi$ obtained under conditions of progressive inhibition of the respiratory chain in the absence of phosphorylation (excess oligomycin), when proton leakage is the only subsystem that consumes $\Delta\Psi$. As a consequence, this relationship also reflects the elasticity of the mitochondrial inner membrane conductance to protons to $\Delta\Psi$.

Oxidation rates were plotted against membrane potential values [34]; the results are presented in Figure 4. Note that the scales for O_2 consumption are different, but that the $\Delta\Psi$ scale is the same at 4, 25 and 37 °C. The relationships between $\Delta\Psi$ and oxidation rate were similar under the different conditions of temperature, and the now classical non-ohmic curve [35] for proton leakage has been obtained at all temperatures studied. However, the shape changed progressively from 37 to 4 °C, becoming steeper. The main consequence was a more rapid decrease of proton leakage for intermediate values of $\Delta\Psi$ when temperature was decreased. In other words, membrane potential showed an increased resistance to the inhibition of respiration at low temperature. The ability of mitochondria incubated at 4 °C

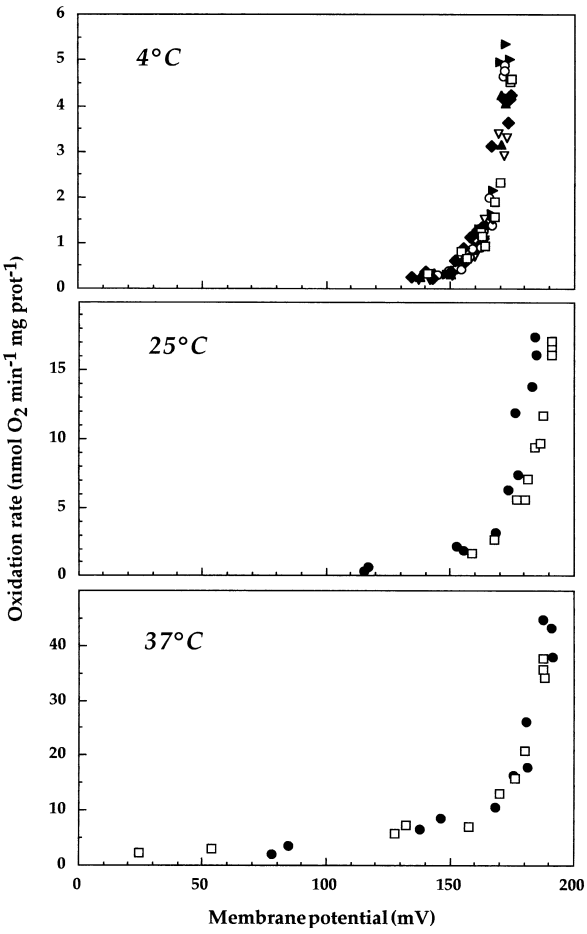

Figure 4 Mitochondrial membrane conductance to protons

Membrane potential and oxidation rates were measured simultaneously during progressive inhibition by malonate (0–18 mM) of the respiratory chain oxidizing succinate (5 mM) in the presence of excess oligomycin (0.5 μg per mg of protein). Experiments were performed on mitochondria incubated at 4 °C (top panel), 25 °C (middle panel) or 37 °C (bottom panel) and data are taken from a total of ten independent mitochondrial preparations (three distinct assays for each experiment).

to generate such a high membrane potential, despite the decrease in oxygen consumption to one-twentieth of that at 37 °C, reflects a huge diminution in the proton conductance of the inner membrane with temperature. As an example, an oxidation rate of 4 nmol O_2 per min per mg protein allows the generation of a maximal membrane potential of 173 mV at 4 °C (Figure 4, top panel), but only of 85 mV at 37 °C (Figure 4, bottom panel). This analysis demonstrates a direct effect of temperature on the mechanism of proton leakage.

Top-down control analysis of oxidative phosphorylation

In the top-down analysis, the proton leakage titration curves presented in Figure 4 allow the calculation of the elasticity of proton leakage to $\Delta\Psi$. Proton leakage is the only subsystem that cannot be measured directly under phosphorylating conditions. However, the strict relationship between proton leakage and $\Delta\Psi$ [33] allows the use of these titrations for the calculation of proton leakage for any given value of $\Delta\Psi$. The elasticity curves of respiration and phosphorylation subsystems to $\Delta\Psi$, as well as

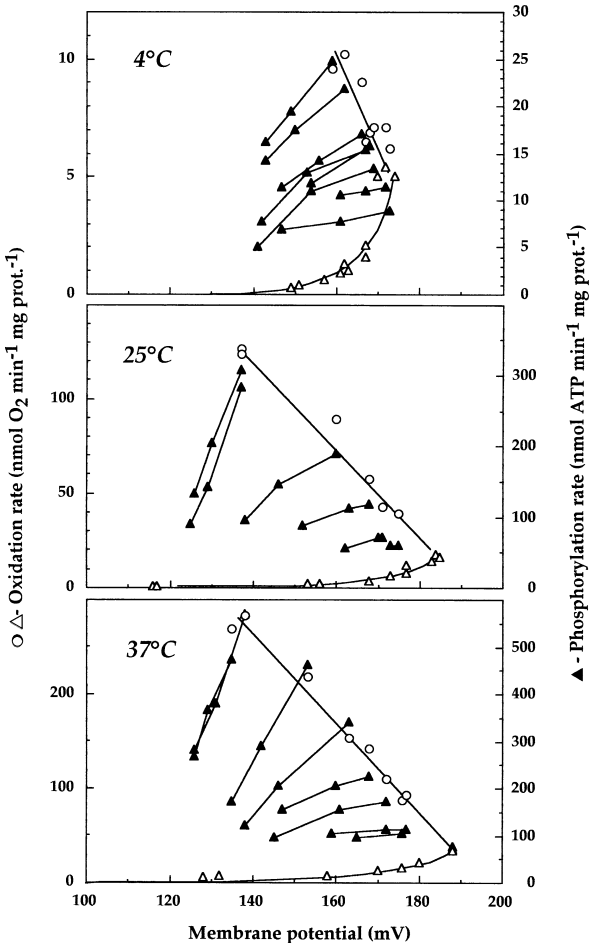

Figure 5 Effect of temperature on the kinetic responses of the different subsystems to $\Delta\Psi$

J_c (○), J_p (▲) and J_l (△) were measured at different $\Delta\Psi$ values during respiration on succinate over a range of conditions between state 4 and state 3 at different temperatures. The different rates of phosphorylation were set up by atractyloside (0–3 μM) in the presence of excess ADP (1 mM). For each temperature, data points come from one typical experiment carried out on a single mitochondrial preparation. Proton leakage elasticity was deduced from the titration of respiration in the absence of phosphorylation. The elasticity coefficients to $\Delta\Psi$ of each subsystem of reactions, and the overall control coefficients, were calculated individually from similar plots of three independent experiments.

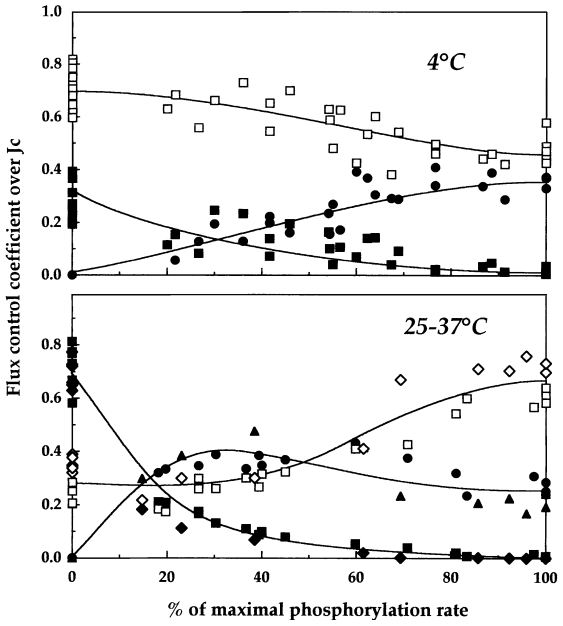

Figure 6 Control coefficients over J_c at different temperatures

Control exerted by the substrate oxidation system (□,◇), the phosphorylation system (●,▲) and proton leakage (■,◆) over the rate of substrate oxidation with succinate as substrate at 4 °C (upper panel), 25 °C and 37 °C (lower panel). Phosphorylation was set at different steady state rates with different concentrations of atractyloside in the presence of excess ADP (1 mM). Data points are taken from three independent experiments.

the different fluxes, were directly determined under stationary conditions as described in the Experimental section.

Figure 5 shows typical experiments used to calculate all the elasticity and control coefficients at each temperature. The relationship between oxidation rate and membrane potential obtained under various phosphorylating conditions set up by atractyloside titration (in Figure 5) describes the elasticity curve for the respiratory chain to $\Delta\Psi$. The elasticity analysis of the phosphorylation subsystem to $\Delta\Psi$ was obtained directly, in contrast with our previous work [13,14], by simultaneously measuring phosphorylation rate and $\Delta\Psi$. This analysis was carried out by titrating $\Delta\Psi$ at each ATP turnover condition with increasing malonate concentrations. Both oxidation and phosphorylation rates were measured during these experiments but only the latter was used for calculations and is presented in Figure 5 (▲); oxidation rate was omitted for the sake of clarity. We observed that temperature lowering affected the elasticities of the three subsystems. Another interesting observation was that phosphorylation occurred for all temperatures around a median of 160 mV. This result emphasized the homoeostasis of the protonmotive force (confirmed below with the top-down control analysis). These data were used to calculate the overall control coefficients of the three subsystems over the different fluxes and over $\Delta\Psi$ [8] presented in the figures below (see the Experimental section for details).

Interestingly, in every phosphorylating condition, no significant difference in the control pattern was found between 25 and 37 °C. This finding was quite surprising, considering the important differences in the oxidation and phosphorylation rates (see Figure 3) as well as in the proton leakage rate (see Figure 4). The distribution of control and therefore the mechanism of the regulation of oxidative phosphorylation seemed unchanged while all parameters were affected. Therefore results obtained at 25 and 37 °C were combined in a single graph for comparison with those obtained at 4 °C.

Figure 6 shows the effect of lowering the temperature on the distribution of control over the rate of oxygen consumption, J_c. The distribution of control coefficients at high temperature (25 or 37 °C; Figure 6, lower panel) was quite similar to published results from Brand and co-workers [7,8,13]. Small differences can be explained by the absence of added hexokinase from our system, this enzyme being part of the phosphorylation subsystem in their experiments and thus participating in control distribution.

At 4 °C the pattern of control distribution was drastically modified. There was a considerable increase in control by substrate oxidation reactions, which exert most of the control on the oxidation rate over the whole range of phosphorylation rates. The remaining control was shared between proton leakages (state 4) and phosphorylation subsystem. This was accompanied by a complete inversion of the distribution of control near state 4; the control shifted from the proton leakage at 25–37 °C to the

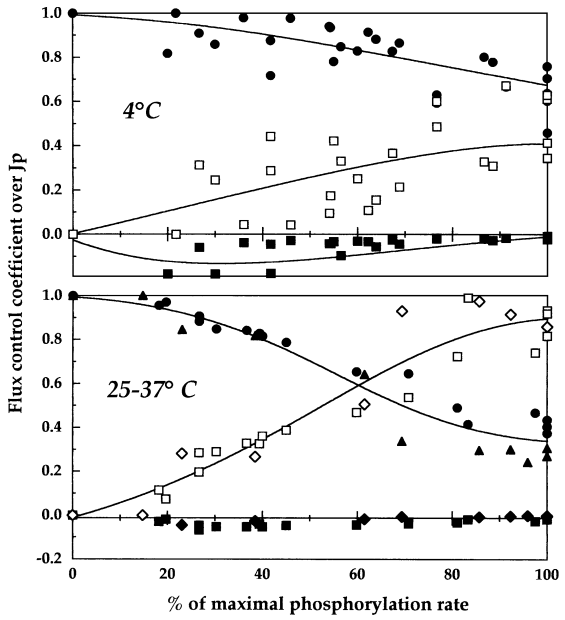

Figure 7 Control coefficients over J_p at different temperatures

Control exerted by the substrate oxidation system (□,◇), the phosphorylation system (●,▲) and proton leakage (■,◆) over the rate of phosphorylation with succinate as substrate at 4 °C (upper panel), 25 °C and 37 °C (lower panel). Conditions as in Figure 5.

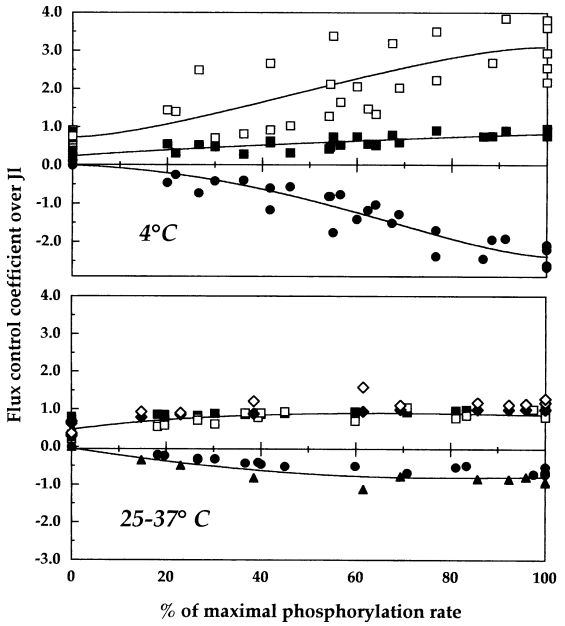

Figure 8 Control coefficients over J_l at different temperatures

Control exerted by the substrate oxidation system (□,◇), the phosphorylation system (●,▲) and proton leakage (■,◆) over the rate of proton leakage with succinate as substrate at 4 °C (upper panel), 25 °C and 37 °C (lower panel). Conditions as in Figure 5.

respiration subsystem at 4 °C. For intermediate ATP turnover, control was exerted mainly by the phosphorylation subsystem at 37–25 °C and by the respiratory chain subsystem at 4 °C. Therefore the more marked difference in the control of the oxidation rate occurred under low and intermediate phosphorylating conditions. The increase in control by the phosphorylation subsystem at 4 °C, as described in [4] for state 3 by using the inhibitor technique, only occurs under conditions very close to state 3.

The distribution of control over the phosphorylation rate is presented in Figure 7. We observed a general increase in control by the phosphorylation subsystem at 4 °C on the rate of ATP synthesis, which exerted most of the control under all phosphorylating conditions. A real decrease in control by the substrate oxidation subsystem is observed only under conditions very close to state 3 at this temperature, in contrast with 25 or 37 °C. However, the control was always shared between the phosphorylation and substrate oxidation subsystems, with almost no control by proton leakage.

Figure 8 shows the flux control coefficients of the three subsystems on proton leakage and is of particular interest for understanding the regulation of phosphorylation efficiency. Owing to the very specific (non-ohmic) relationship between proton leakage rate and membrane potential, very high values of control coefficients on proton leakage rate were measured. These values are positive for the respiratory chain and the leakage subsystem and negative for the phosphorylation subsystem. The negative values represent the negative (inhibitory) effect of phosphorylation on the leaks: the increase in ATP synthesis leads to a decrease in $\Delta\Psi$, which is responsible for the decrease in leak rate. This phenomenon was considerably enhanced at low temperature, and negative control coefficients close to -3.0 were measured. These results are the consequence of the important changes in the elasticity curves of the proton leakage to $\Delta\Psi$ at 4 °C (see Figures 4 and 5).

By comparison, the concentration control coefficients of the different subsystems on the value of $\Delta\Psi$ presented in Figure 9 were very small. This result has been obtained for all top-down metabolic control analyses carried out so far, and appears as a

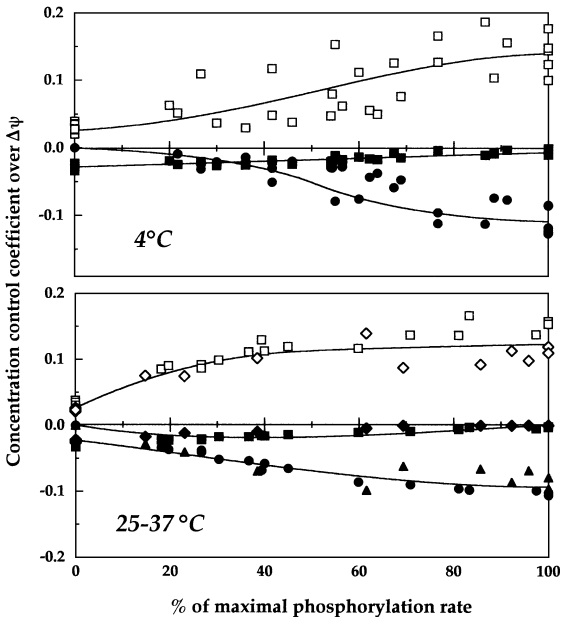

Figure 9 Control coefficients over $\Delta\Psi$ at different temperatures

Control exerted by the substrate oxidation system (□,◇), the phosphorylation system (●,▲) and proton leakage (■,◆) over $\Delta\Psi$ with succinate as substrate at 4 °C (upper panel), 25 °C and 37 °C (lower panel). Conditions as in Figure 5.

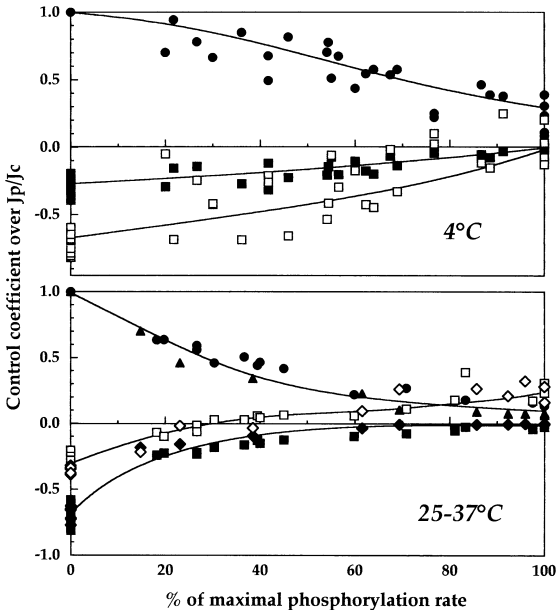

Figure 10 Control coefficients over the ATP/O ratio at different temperatures

Control exerted by the substrate oxidation system (□,◇), the phosphorylation system (●,▲) and proton leakage (■,◆) over the ATP/O ratio with succinate as substrate at 4 °C (upper panel), 25 °C and 37 °C (lower panel). Conditions as in Figure 5.

constant feature of mitochondrial function. Some variations were observed through the range of ATP turnover but values always remained below 0.2 in absolute value. The shapes were slightly modified but we can almost superimpose the two graphs of Figure 9.

Under physiological conditions, one of the most important parameters with $\Delta\Psi$ is the apparent efficiency of phosphorylation, expressed as the effective ATP/O ratio. This ratio increases as the phosphorylation rate increases and approaches the mechanistic ATP/O ratio under state 3 conditions, where proton leakage is minimized. In state 4, there is no net ATP synthesis and all the proton current is via the leakage pathway; therefore the effective ATP/O ratio is zero [16]. The increase in phosphorylation rate is linked to the decrease in the proton leakage rate via the decrease in $\Delta\Psi$ (see Figure 5). The control exerted by the different subsystems on the ATP/O ratio can be calculated from the analysis presented in Figures 6 and 7. For each subsystem the control exerted over the ATP/O ratio is the difference between the control over J_p (Figure 7) and over J_c (Figure 6), as the effective ATP/O ratio at the steady state is the ratio of the fluxes of phosphorylation and substrate oxidation [16] (see the Experimental section). These control coefficients reflect the global effect of each subsystem on the effective efficiency of phosphorylation.

The negative control by the proton leakage subsystem was low under all ATP turnover conditions except close to state 4 (Figure 10); under phosphorylating conditions the pattern was not markedly affected by the change in temperature. The main changes observed concerned the two other subsystems: the general increase in positive control by the phosphorylation subsystem was compensated for by a general increase in negative control by the respiratory chain subsystem. Positive control by the phosphorylation subsystem reflects the fact that any increase in phosphorylation activity causes an increase in the ATP/O ratio. The other interesting result is the increase in absolute value of the negative control by the respiratory chain on the ATP/O ratio at 4 °C, indicating that an increase in substrate supply, for example, would cause a decrease in the ATP/O ratio, i.e. a greater increase in the leakage pathway than in the phosphorylation reactions. These results are the direct consequence of the changes in the elasticity of the proton leakage towards the membrane potential and of the fact that the proton leakage rate was higher under all phosphorylating conditions at 4 °C. In comparison with high temperatures, the whole pattern of control indicates that the efficiency of phosphorylation becomes highly sensitive to all changes in conditions.

Conclusions

The analysis presented here was designed to study the effect of a complex effector, i.e. temperature, on oxidative phosphorylation. Succinate was chosen because it seemed significant and therefore gives a valid picture of how control is distributed [16]. It was shown that the overall reaction rates were greatly reduced with temperature, as previously observed [5,6,36], whereas maximal membrane potential was only slightly affected at 4 °C. Interestingly, the classical parameters of mitochondrial integrity (respiratory control and ATP/O ratios) did not follow this temperature variation (see Figure 3) and presented a maximum at 25 °C, well below the physiological value of 37 °C (see also [6]). As previously demonstrated [32,37], the increase in state 3 membrane potential value between 25 and 4 °C is sufficient to explain the decrease in phosphorylation efficiency at 4 °C: the decrease in depolarization can be ascribed only to a relative inhibition of the phosphorylation flux and is responsible for an increase in the proton leakage flux [32,37]. The picture was very different when we compared 25 °C with 37 °C, because depolarization was almost unchanged: no clear explanation emerged from these results. We could, however, make a parallel with our previous observation that depolarization was not modified when mitochondria were progressively uncoupled, indicating that changes in inner mitochondrial membrane conductance to protons do not affect depolarization [32].

Top-down elasticity analysis of the proton leakage reactions towards membrane potential values gave additional useful information. The proton leakage rate decreased drastically with temperature, even though comparable maximal values of membrane potential were maintained. However, the dependence of proton leakage on membrane potential was progressively modified (Figure 4): the main change observed was a relative increase in leakage rate for intermediate and low values of membrane potential when temperature increased (see Figure 4). This progressive change in membrane conductance to protons with temperature (no drastic change was observed here) explains the surprising change of the ATP/O ratio between 25 °C and 37 °C by an increase in the leakage rate at equivalent protonmotive force.

Top-down control analysis was, however, necessary for understanding the complex effect of temperature and for identifying the main sites of its action on oxidative phosphorylation over the total range of ATP synthesis. The complete analysis led to another important result: despite the large differences in all activities as well as phosphorylation efficiency, the patterns of control seemed strictly identical between 37 and 25 °C under all phosphorylating conditions. Therefore the differences observed at 4 °C cannot be ascribed solely to the drastic decrease in mitochondrial activities but must be due also to a relative decrease in activities or changes in elasticities of the subsystems to $\Delta\Psi$. Temperature affected all mitochondrial properties studied

here, as well as the three subsystems activities, as shown by elasticity analyses (see Figure 5). The changes in membrane conductance to protons with temperature did not seem to play a crucial role because they affected neither the protonmotive force nor the control pattern. Top-down control analysis clearly showed that the other subsystems were both responsible for the changes in the control pattern at 4 °C, depending on the activity of the mitochondria. Under state 3 conditions, the relative inhibition of the phosphorylation subsystem prevailed. However, the control pattern on J_e clearly indicates that a modification of the substrate oxidation subsystem was predominant under all other conditions, including state 4.

We thank Dr. E. Thiaudière and B. Quesson for their help with the mathematical treatment of the data.

REFERENCES

1 Ogawa, S., Rottenberg, H., Brown, T. R., Shulman, R. G., Castillo, C. L. and Glynn, P. (1978) Proc. Natl. Acad. Sci. U.S.A. **75**, 1796–1800
2 Hutson, S. M., Berkich, D. A., Williams, G. D., LaNoue, K. F. and Briggs, R. W. (1989) Biochemistry **28**, 4325–4332
3 Hutson, S. M., Williams, G. D., Berkich, D. A., LaNoue, K. F. and Briggs, R. W. (1992) Biochemistry **31**, 1322–1330
4 Quentin, E., Avéret, N., Guérin, B. and Rigoulet, M. (1994) Biochem. Biophys. Res. Commun. **202**, 816–821
5 Rottenberg, H. (1978) FEBS Lett. **94**, 295–297
6 Rottenberg, H., Robertson, D. E. and Rubin, E. (1985) Biochim. Biophys. Acta **809**, 1–10
7 Brown, G. C., Hafner, R. P. and Brand, M. D. (1990) Eur. J. Biochem. **188**, 321–325
8 Hafner, R. P., Brown, G. C. and Brand, M. D. (1990) Eur. J. Biochem. **188**, 313–319
9 Brand, M. D., Chien, L.-F., Ainscow, E. K., Rolfe, D. F. S. and Porter, R. K. (1994) Biochim. Biophys. Acta **1187**, 132–139
10 Brand, M. D. and Brown, G. C. (1994) in Biothermokinetics (Westerhoff, H. V., ed.), pp. 27–35, Intercept Ltd, Andover
11 Brand, M. D., Chien, L.-F. and Rolfe, D. F. S. (1993) Biochem. Soc. Trans. **21**, 757–762
12 Buttgereit, F., Grant, A., Müller, M. and Brand, M. D. (1994) Eur. J. Biochem. **22**, 513–519
13 Kesseler, A., Diolez, P., Brinkmann, K. and Brand, M. D. (1992) Eur. J. Biochem. **210**, 775–784
14 Diolez, P., Kesseler, A., Haraux, F., Valerio, M., Brinkmann, K. and Brand, M. D. (1993) Biochem. Soc. Trans. **21**, 769–773
15 Westerhoff, H. V. and van Dam, K. (1987) Thermodynamics and Control of Biological Free-Energy Transduction, Elsevier, Amsterdam
16 Brand, M. D., Harper, M.-E. and Taylor, H. C. (1993) Biochem J. **291**, 739–748
17 Nobes, C. D., Brown, G. C., Olive, P. N. and Brand, M. D. (1990) J. Biol. Chem. **265**, 12903–12909
18 Harper, M.-E. and Brand, M. D. (1993) J. Biol. Chem. **268**, 14850–14860
19 Kesseler, A. and Brand, M. D. (1994) Eur. J. Biochem. **225**, 897–906
20 Kesseler, A. and Brand, M. D. (1994) Eur. J. Biochem. **225**, 907–922
21 Kesseler, A. and Brand, M. D. (1994) Eur. J. Biochem. **225**, 923–935
22 Cannon, B. and Lindberg, O. (1979) Methods Enzymol. **60**, 65–78
23 Estabrook, R. W. (1967) Methods Enzymol. **10**, 40–47
24 Kamo, N., Muratsugu, M., Hongoh, R. and Kobatake, Y. (1979) J. Membr. Biol. **81**, 127–138
25 Goubern, M., Yazbeck J., Chapey, M.-F., Diolez, P. and Moreau, F. (1990) Biochim. Biophys. Acta **1015**, 334–340
26 Thiaudière, E., Gallis, J.-L., Dufour, S., Rousse, N. and Canioni, P. (1993) FEBS Lett. **330**, 231–235
27 Nishimura, M., Ito, T. and Chance, B. (1962) Biochim. Biophys. Acta **59**, 177–182
28 Bradford, M. M. (1976) Anal. Biochem. **72**, 248–254
29 Kacser, H. and Burns, J. A. (1973) Symp. Soc. Exp. Biol. **32**, 65–105
30 Heinrich, R. and Rapoport, T. A. (1974) Eur. J. Biochem. **42**, 89–95
31 Fell, D. A. and Sauro, M. (1985) Eur. J. Biochem. **148**, 555–561
32 Diolez, P. and Moreau, F. (1985) Biochim. Biophys. Acta **806**, 56–63
33 Brand, M. D., Chien, L.-F. and Diolez, P. (1994) Biochem. J. **297**, 27–29
34 Brand, M. D. and Diolez, P. (1993) in Modern Trends in Biothermokinetics (Schuster, S. and Nazat, J. P., eds.), pp. 333–338, Plenum Press, New York
35 Nicholls, D. G. (1974) Eur. J. Biochem. **50**, 305–315
36 Thayer, W. S. and Rubin, E. (1981) J. Biol. Chem. **256**, 6090–6097
37 Diolez, P. and Brand, M. D. (1992) In Molecular, Biochemical, and Physiological Aspects of Plant Respiration (Lambers, H. and van der Plas, L. H. W., eds.), pp. 93–100, SPB Academic Publishing, The Hague

Received 3 July 1995/4 October 1995; accepted 31 October 1995